

An exact real-space renormalization method and applications

Adrian E. Feiguin,^{1,*} Rolando D. Somma,² and Cristian D. Batista²

¹*Department of Physics, Northeastern University, Boston, MA 02115, USA.*

²*Theory Division, Los Alamos National Laboratory, Los Alamos, NM 87545, USA.*[†]

(Dated: October 31, 2019)

We present a numerical method based on real-space renormalization that outputs the exact ground space of “frustration-free” Hamiltonians. The complexity of our method is polynomial in the degeneracy of the ground spaces of the Hamiltonians involved in the renormalization steps. We apply the method to obtain the full ground spaces of two spin systems. The first system is a spin-1/2 Heisenberg model with four-spin cyclic-exchange interactions defined on a square lattice. In this case, we study finite lattices of up to 160 spins and find a triplet ground state that differs from the singlet ground states obtained in C.D. Batista and S. Trugman, *Phys. Rev. Lett.* **93**, 217202 (2004). We characterize such a triplet state as consisting of a triplon that propagates in a background of fluctuating singlet dimers. The second system is a family of spin-1/2 Heisenberg chains with uniaxial exchange anisotropy and next-nearest neighbor interactions. In this case, the method finds a ground-space degeneracy that scales quadratically with the system size and outputs the full ground space efficiently. Our method can substantially outperform methods based on exact diagonalization and is more efficient than other renormalization methods when the ground-space degeneracy is large.

I. INTRODUCTION

Renormalization methods are powerful tools for studying the long-wavelength properties of physical systems by a systematic elimination of high-energy degrees of freedom. The first numerical renormalization group (NRG) method was developed by Wilson [1, 2] to solve the Kondo problem, an important problem in physics that involves the interaction of a magnetic impurity with a conduction band [3]. The more recent density-matrix renormalization group (DMRG) method was successfully applied to a large class of one-dimensional ($D = 1$) quantum systems [4] and a few $D = 2$ systems [5–8]. Recent advances in quantum information theory also led to renormalization and variational methods, including PEPS [9, 10], MERA [11, 12], and tensor renormalization [13–16]. The problem with known renormalization methods is that they suffer from important limitations when studying systems in space dimension $D \geq 2$ or with a large number of ground states. Our goal is to construct a renormalization method that can be applied to such systems when the Hamiltonians under consideration satisfy a “frustration-free” (FF) property.

The term “frustration free” was first coined by the quantum-information community [18–20] to denote a class of Hamiltonians $H = \sum_{k=1}^P \pi_{v_k}$ whose ground states are also ground states of each local term π_{v_k} . v_k refers to a finite set of degrees of freedom, e.g., a unit or a finite subsystem. While describing such Hamiltonians as FF is adequate from a viewpoint that we discuss below, the term FF can be confusing if we adopt a more traditional convention of identifying frustration with competing interactions. For example, the triangular lattice Ising model with antiferromagnetic (AFM) exchange ($J > 0$) is the paradigmatic example of a frustrated Hamiltonian. However, this model is FF according to the previous defini-

tion. We let v_k be the three spins $\sigma_j^k = \{-1, 1\}$ in the k th triangle, $j = \{1, 2, 3\}$, and define $\pi_{v_k} = (J/2)[(\sum_j \sigma_j^k)^2 - 1]$. The Hamiltonian is FF because any ground state $|\psi\rangle$ of H satisfies $\pi_{v_k}|\psi\rangle = 0$, i.e., $|\psi\rangle$ is also a ground state of each π_{v_k} . Nevertheless, $|\psi\rangle$ does not *minimize* each of the bond Hamiltonians $J\sigma_j^k\sigma_{j'}^k$, reason why the model is considered to be frustrated according to the traditional convention.

The previous discussion implies that the concept of frustration is relative to a particular decomposition of H . The traditional interpretation of frustration assumes a decomposition of H dictated by the physical nature of the interactions. However, while H may be frustrated with respect to one decomposition, it may still be FF because the competition between interactions on different units disappears when we consider a different decomposition (e.g., triangles instead of bonds in the Ising example). Remarkably, FF Hamiltonians are ubiquitous in condensed matter and quantum information theory. They include Ising models, the AKLT model [21], parent Hamiltonians of PEPS [9], and Hamiltonians that can simulate quantum circuits [22]. Several other frustrated magnets also correspond to FF Hamiltonians [23]. Ground states of FF Hamiltonians contain all the characteristics of highly frustrated physical systems: large ground state degeneracy [24], coexistence of different phases, and exotic orderings.

In this manuscript, we introduce an exact real-space renormalization method (ERM) that obtains the full ground-space of FF Hamiltonians. The output of the ERM is a sequence of tensors whose contraction allows us to compute expectation values of observables and amplitudes of the ground states (Sec. II). The computational cost of our method (i.e., the cost of the tensor contraction) is polynomial in the ground-space degeneracy of the FF Hamiltonians involved in the renormalization steps. If such a degeneracy increases polynomially with the system size, the ERM is efficient. Otherwise, for exponentially large degeneracies, the ERM is inefficient but can substantially outperform other numerical techniques for this problem.

To illustrate the potential of our method, we apply it to two FF spin systems that have largely degenerate ground states.

* a.feiguin@neu.edu

† somma@lanl.gov

The first system is a spin-1/2 Heisenberg model with four-spin cyclic-exchange interactions that is defined on a square lattice (Sec. III). The ground state degeneracy is exponential in the linear size, L , of the lattice. Such a degeneracy is much smaller than the Hilbert space dimension 2^{L^2} , so the ERM outperforms exact diagonalization in this case. Besides the singlet ground states that were identified in Ref. [25], we find a triplet ground state that consists of a triplon that propagates in a background of fluctuating singlet dimers. The propagation of this triplon leads to an incipient long range AFM ordering, which indicates that the triplet ground state describes an AFM quantum critical point. Such a triplet ground state also exists in rectangular spin lattices of size $L_x \times L_y$, $L_x \leq L_y$, with periodic boundary conditions. In particular, Lajkó, Sindzingre, and Penc, gave an analytical expression of this state for the case of three-leg tubes ($L_x = 3$) [26].

The second of system consists of the family of spin-1/2 Heisenberg chains with uniaxial exchange anisotropy and nearest and next-nearest-neighbor exchange interactions (Sec. IV). The Hamiltonians in this family are also FF. An analytical and closed form representation for the ground states of this family, in terms of anyonic operators, was given in Ref. [23]. However, such a representation may not be useful for computing some expectation values of spin-spin correlations efficiently. Those expectation values can be efficiently computed with the ERM.

We note that quantum Monte Carlo methods, that are not based on renormalization, cannot be applied to most FF Hamiltonians because of the infamous sign problem.

II. THE RENORMALIZATION METHOD

We start by providing a brief description of the ERM (technical details are provided in Appendix A). For simplicity, we consider a Hamiltonian H acting on a system of L spins located on the vertices \mathcal{V} of a lattice [30]. The Hilbert space of the system is $\mathcal{H}_{\mathcal{V}}$ and its dimension is $d_{\mathcal{V}}$. The magnitude of the spins and space dimensionality of the lattice are arbitrary; we refer to the spin system of Fig. 1 for illustration purposes. We let v_k be a subset of spins of \mathcal{V} , \mathcal{H}_k the associated Hilbert space, and d_{v_k} its dimension. Here, $k = 1, 2, \dots, p$ and the subsets v_k are known. For $l = 1, 2, \dots, p$ we also define the sets of spins $w_l = v_l \setminus z_{l-1}$, with $z_l = \bigcup_{k=1}^l v_k = \bigcup_{k=1}^l w_k$ and $z_0 = \{\emptyset\}$. $A \setminus B$ is the relative complement of A in B so that w_l are those spins that belong to v_l but do not belong to any other v_k with $1 \leq k \leq l-1$. We assume $w_l \neq \{\emptyset\}$ and note that $v_1 = w_1 = z_1$.

For a set x of spins in \mathcal{V} , we use i^x for the spin variable in some standard basis [32]. Also, d_x denotes the dimension of \mathcal{H}_x , the Hilbert space associated with x . It follows that $\{|i^x\rangle\}_{1 \leq i^x \leq d_x}$ is an orthonormal basis for the spins in x ; hereafter referred to as the computational basis and $|i^x\rangle$ is a basis state. In some cases, we do not distinguish between basis states or (column) vectors: $|i^x\rangle$ can also denote a vector with component equal to 1 in position i^x and zeroes elsewhere. The number of components of $|i^x\rangle$ is the number of values that i^x can take ($\leq d_x$), which is given in each case.

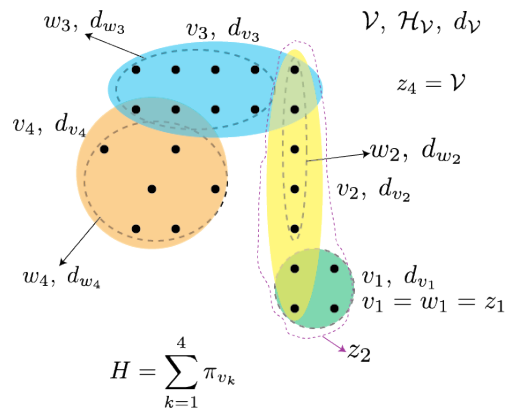


FIG. 1. Spin system. Black dots denote spins located at the vertices \mathcal{V} of the lattice. Each term π_{v_k} in the Hamiltonian acts nontrivially in v_k only. The sets w_l and z_l are defined in the text.

The Hamiltonian is represented as

$$H = \sum_{k=1}^p \pi_{v_k}, \quad (1)$$

where each π_{v_k} is a Hermitian operator acting nontrivially on spins in v_k only. We assume $\pi_{v_k} \geq 0$. If any ground state $|\psi\rangle$ of H satisfies

$$H|\psi\rangle = \pi_{v_1}|\psi\rangle = \dots = \pi_{v_p}|\psi\rangle = 0, \quad (2)$$

then H is said to be FF. The standard definition of FF also assumes that each π_{v_k} is local. Here, we can relax such an assumption without incurring in large computational overheads as long as π_{v_k} is a bounded sum of product operators (see Appendix A). When H is FF, our renormalization method is *exact* and outputs the ground states of H as

$$|\psi_{i^{\mathcal{V}}}^p\rangle = T_1^\dagger \bullet \dots \bullet T_p^\dagger |i^{\mathcal{V}}\rangle. \quad (3)$$

$T_1^\dagger, T_2^\dagger, \dots, T_p^\dagger$ are isometries, $1 \leq i^{\mathcal{V}} \leq g$, and g is the ground-space dimension. The symbol \bullet refers to a tensor contraction that involves a sum over repeated indices. Such a contraction regards a tree-tensor network (see Fig. 2); Tree-tensor networks are ubiquitous in renormalization methods [33, 34]. Whether H is FF or not is also an output of the ERM.

The ERM performs p steps. Each step can be defined recursively as follows. For $1 \leq l \leq p$, we let $g_l \geq 0$ be the ground-space degeneracy of $H_l = \sum_{k=1}^l \pi_{v_k}$ ($g_0 = 1$). The ground states of H_l are $|\psi_{i^{z_l}}^l\rangle$, $1 \leq i^{z_l} \leq g_l$. $H_p = H$. In the first step, the ERM diagonalizes γ_1 , the $d_{w_1} \times d_{w_1}$ matrix representation of π_{v_1} in the computational basis. It obtains g_1 and $\{|\psi_{i^{z_1}}^1\rangle\}_{1 \leq i^{z_1} \leq g_1}$, and continues only if $g_1 > 0$. In the l -th step, $l \geq 2$, the ERM computes γ_l . This is a $h_l \times h_l$ matrix representation of π_{v_l} in the basis $\{|\psi_{i^{z_{l-1}}}^{l-1}, i^{w_l}\rangle\}$, with $1 \leq i^{z_{l-1}} \leq g_{l-1}$, $1 \leq i^{w_l} \leq d_{w_l}$, and $h_l = g_{l-1} d_{w_l}$. Then ERM applies exact diagonalization to γ_l , obtains a basis $\{|\psi_{i^{z_l}}^l\rangle\}$ for the zero eigenvalue, and computes the multiplicity g_l of the new ground space. The ERM continues only if

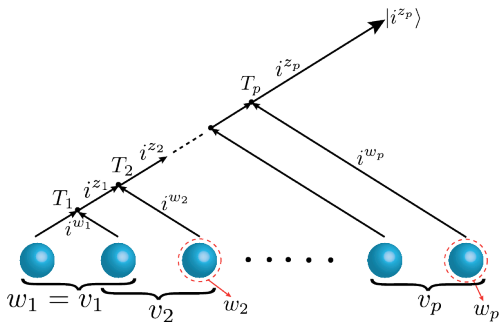


FIG. 2. Representation of the tree-tensor network contraction for a system with p spins (blue circles). In this example, the sets v_l refer to pairs of nearest-neighbor spins and each w_l is a single spin. The tensors T_l live in the vertices of the tree and the contraction indices are in the edges. An arrow means a sum over the corresponding index. The contraction $T_p \bullet \dots \bullet T_1$ maps ground states of H into states $|i^{z_p}\rangle$. $T_1^\dagger \bullet \dots \bullet T_p^\dagger$ is the inverse transformation that gives all the ground states of H from $|i^{z_p}\rangle$.

$g_l > 0$. The isometries in Eq. (3) are

$$T_l^\dagger = \sum_{i^{z_l}=1}^{g_l} |\psi_{i^{z_l}}^l\rangle \langle i^{z_l}|. \quad (4)$$

In Appendix A we show that, if N_T is the number of elementary operations to output the isometries $T_1^\dagger, \dots, T_p^\dagger$, then

$$N_T \propto \sum_{k=1}^p EV(h_k) + (p-k)(h_k g_k)^2. \quad (5)$$

$EV(d)$ is the cost of the exact diagonalization of a $d \times d$ matrix and $g_0 = 1$. Also, if M_T is the memory cost associated with the number of variables kept during the implementation of the ERM,

$$M_T \propto \sum_{k=1}^p h_k g_k. \quad (6)$$

Thus, the efficiency of the ERM strongly depends on g_k and the method becomes efficient when $g_k \in \mathcal{O}[\text{poly}(p)]$. The cost of evaluating expectation values of observables in any ground state of H is also important and can be easily derived from the analysis given in Appendix A.

A related method for solving some spin-1/2 systems, which is based on the techniques developed in Ref. [27], can be found in Ref. [28]. Also, an exact renormalization method for quantum spin chains was proposed in Ref. [29]. Our main contribution with respect to that of Refs. [28, 29] is that we consider Hamiltonians with arbitrary interactions, in any space dimension, and provide a real-space renormalization algorithm that is exact if the ground space satisfies some properties that can be verified by the ERM. In addition, the way that the ERM contracts tensors is different from the usual contraction of a binary-tree like tensor network. The main reason behind this difference is the minimization of M_T when g_l grows monotonically with l .

III. APPLICATION TO A $D = 2$ MAGNET

A. Model Hamiltonian

We apply the ERM to a spin-1/2 model that satisfies the frustration-free property as defined in Sec. II. The FF Hamiltonian is defined on a square lattice and reads [25]:

$$H = \frac{3}{2} \sum_{\alpha} \mathcal{P}^{\alpha}. \quad (7)$$

Each operator \mathcal{P}^{α} projects the total spin state of a square plaquette α onto the subspace with spin 2, as illustrated in Fig.3(a). This model has a number of exact valence-bond ordered ground states that increases exponentially in the linear dimension of the square lattice [25]. The model of Eq. (7) corresponds to a particular regime of parameters of a more general model with frustration and ring exchange:

$$H' = J_1 \sum_{\langle \mathbf{r}, \mathbf{r}' \rangle} \mathbf{s}_{\mathbf{r}} \cdot \mathbf{s}_{\mathbf{r}'} + J_2 \sum_{\langle\langle \mathbf{r}, \mathbf{r}' \rangle\rangle} \mathbf{s}_{\mathbf{r}} \cdot \mathbf{s}_{\mathbf{r}'} + K \sum_{\alpha} (P_{ij}^{\alpha} P_{kl}^{\alpha} + P_{jk}^{\alpha} P_{il}^{\alpha} + P_{ik}^{\alpha} P_{jl}^{\alpha}). \quad (8)$$

Here, $\langle \mathbf{r}, \mathbf{r}' \rangle$ and $\langle\langle \mathbf{r}, \mathbf{r}' \rangle\rangle$ denote nearest neighbors and next nearest neighbors, respectively, and i, j, k , and l label the four spins of a plaquette in cyclic order. $\mathbf{s}_{\mathbf{r}} = (s_{\mathbf{r}}^x, s_{\mathbf{r}}^y, s_{\mathbf{r}}^z)$ is the spin operator of the spin at the \mathbf{r} th position. Equation (7) reduces to Eq. (8), up to an irrelevant constant, if $J_1 = 1$, $J_2 = 1/2$, and $K = 1/8$. This case corresponds to the maximally frustrated point as a function of J_2/J_1 .

B. Algorithm

The implementation of the ERM is related to Wilson's NRG [1, 2] and to the warmup stage of the conventional DMRG [4]. Thus, it is simple to adapt an existing NRG or DMRG code for this case by making minor modifications. At each renormalization step, the ERM *grows* the system by adding one plaquette. Then, the ERM diagonalizes the renormalized Hamiltonian and only keeps the ground states (if the lowest eigenvalue is zero). In a DMRG “language”, this corresponds to working with two blocks instead of four.

The order in which the plaquettes are added can be arbitrary. However, the ground space degeneracy, g_l , depends dramatically on the path followed to grow the lattice. The “snake” path shown in Fig. 3(b) is the approach that turned out to be more efficient. The number of spins increases by one or by two at each step [see for instance steps 5 and 6 in Fig. 3(b)]. It is important to introduce Hamiltonian terms corresponding to a plaquette at a time (the projectors \mathcal{P}^{α}) and to avoid including terms belonging to neighboring plaquettes. For instance, a nearest neighbor exchange term in Eq. (8) is shared by two neighboring plaquettes. Such a term should be split accordingly to assure that only one projector is added per step.

We applied the ERM to rectangular lattices of sizes $L_x \times L_y$, $L_x \leq L_y$, and periodic boundary conditions. The ground

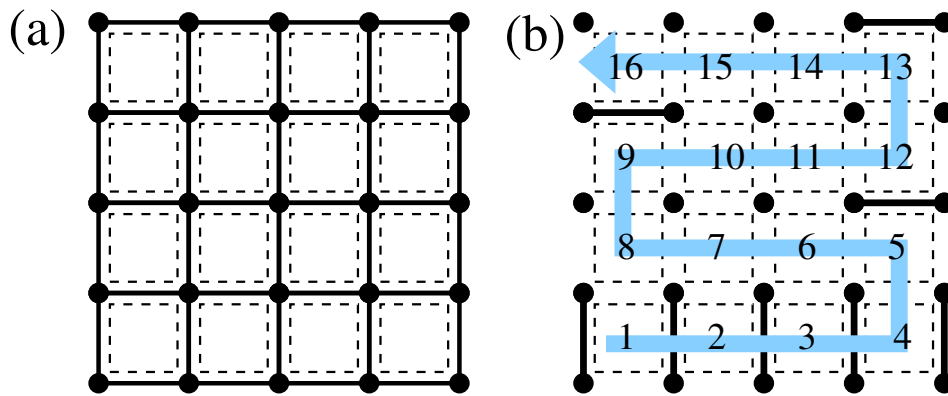


FIG. 3. (Color online) (a) Square lattice and the projectors \mathcal{P}^α acting on the square plaquettes (dashed lines). Each \mathcal{P}^α projects the spin states of the plaquette onto the subspace with spin 2. (b) “Snake” path followed by the ERM, similar to the DMRG warmup scheme. At each step one adds the spins necessary to complete a projector on a new plaquette. This growing process requires adding one or two spins (thick bold lines) per step.

space degeneracy g is proportional to 2^{L_x} in this case, i.e. exponential in the linear dimension. If we follow a path like the “snake” in Fig. 3(b), g_l increases as we increase L_x but it does not change substantially when we increase L_y . This property allows us to study remarkably large system sizes by keeping L_x constant and by increasing the number of plaquettes in the y direction to relatively large values of L_y . Every time we close a boundary along the y direction, the degeneracy g_l drops substantially.

Unlike DMRG, the ERM needs to fully diagonalize the renormalized Hamiltonian at each step. This implies diagonalizing a $h_l \times h_l$ matrix in the l th step, with $h_l = 2g_{l-1}$ or $h_l = 4g_{l-1}$, depending on the number of spins added at that step (one or two, respectively). The maximum value of h_l depends on the linear dimensions of the system, and could reach several thousands for lattices of hundreds of spins. To be able to study relatively large systems, we can use symmetries –U(1)/abelian quantum numbers in our case– to store the Hamiltonians and other operators in block form. However, to ensure that we keep all the ground states, we do not restrict the values of these quantum numbers.

In Fig. 4 we plot the ground-space degeneracy, g_l , and order of the renormalized Hamiltonian, h_l , for a 6×6 lattice ($L_x = L_y = 6$). We also plot the order of the largest block in the renormalized Hamiltonian when symmetries are considered, h_l^{\max} , which determines the dominating cost of the method. The oscillation in g_l has a periodicity corresponding to the linear dimension of the lattice, showing the reduction in the ground space degeneracy every time a lattice boundary is closed.

Because we are interested in the computation of correlation functions of arbitrary ground states, at each step we need to store all the matrices of the operators involved in such correlations. We note that correlators of the form $\langle AB \rangle$ cannot be computed by storing the operators A and B independently. In general, it is necessary to store the matrices for the product AB because the product of two projected operators is not equal to the projection of the product.

The ground states of H can be obtained for 8×8 and larger

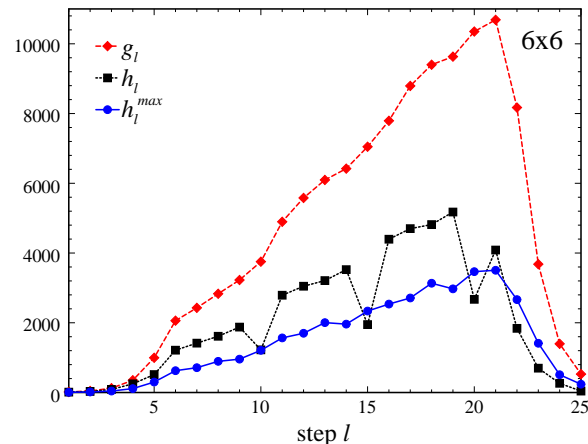


FIG. 4. Ground space degeneracy (g_l), order of the renormalized Hamiltonian (h_l), and order of the largest block in the renormalized Hamiltonian (h_l^{\max}) per step of the ERM, when symmetries are considered.

lattices by implementing the ERM on more powerful existing computers. The requirement of storing all the operators associated with the correlations described in the next section and those needed for computing the Hamiltonian terms, is the main limiting factor for increasing the lattice size.

C. Results

In addition to the large set of exact $S = 0$ ground states exhibiting valence bond ordering [25], the results output by the ERM show a triplet ground state, with $S = 1$, $S^z = \pm 1, 0$. (S is the total spin of the lattice and S^z the z th component of the total spin.) Such a state was also identified by exact diagonalization of small square clusters and by an analytical solution of the model on $3 \times L_y$ tubes [26, 35]. That the $S = 1$ state exists in larger systems was unexpected and illustrates the importance of methods that obtain the full ground space. The

existence of a triplet ground state is compatible with a critical scenario in which H has a gapless spectrum of $S = 1$ spin excitations. In this case, an external magnetic field $B > 0$ would induce AFM ordering of the spin components that are orthogonal to the field's direction. This scenario is confirmed by the spin-spin correlators obtained with our ERM for the $S = S^z = 1$ ground state on $4 \times L_y$ and $6 \times L_y$ finite lattices. Figure 5 shows the two-point correlators $\langle s_0^z s_r^z \rangle$ and $\langle s_0^+ s_r^- \rangle$ as a function of the distance along the y -direction. $\mathbf{0} = (0, 0)$ denotes a reference spin (the origin), $\mathbf{r} = (0, y)$, and $s_r^\pm = s_r^x \pm i s_r^y$. While there is a clear long-range AFM tail for $\langle s_0^+ s_r^- \rangle$, the $\langle s_0^z s_r^z \rangle$ correlator decays exponentially in r . It is important to note that the magnitude of the local staggered xy -magnetization is of order $1/\sqrt{L_x L_y}$, which is the expected behavior for the condensation of a single triplon. This property is revealed by the scaling behavior of the structure factor,

$$S^\pm(\mathbf{k}) = \frac{1}{L_x L_y} \sum_{\mathbf{r}, \mathbf{r}'} e^{i\mathbf{k} \cdot (\mathbf{r} - \mathbf{r}')} \langle s_{\mathbf{r}}^+ s_{\mathbf{r}'}^- \rangle, \quad (9)$$

evaluated at the AFM wave vector $\mathbf{k} = (\pi, \pi)$ (inset of Fig. 5). $S^\pm(\pi, \pi)$ tends to a value of order one for $L_x, L_y \rightarrow \infty$, indicating that the order parameter $\frac{1}{L_x L_y} \sum_{\mathbf{r}} e^{i\mathbf{k} \cdot \mathbf{r}} s_{\mathbf{r}}^\nu$, $\nu = \{x, y\}$, is proportional to $1/\sqrt{L_x L_y}$.

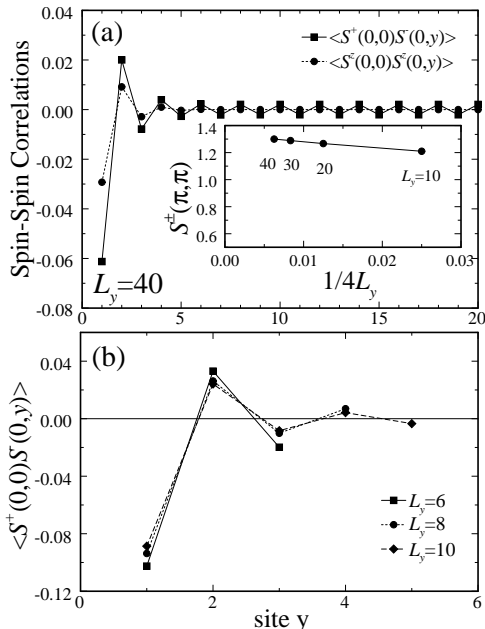


FIG. 5. Two-point correlators $\langle s_0^z s_r^z \rangle$ and $\langle s_0^+ s_r^- \rangle$ as a function of distance along the y -direction. Here, $\mathbf{0}$ is a spin of reference and $\mathbf{r} = (0, y)$. The figure shows the correlations for a) $4 \times L_y$ and b) $6 \times L_y$ lattices. Inset of a): scaling of the structure factor, $S^\pm(\mathbf{k})$, evaluated at the AFM wave vector $\mathbf{k} = (\pi, \pi)$.

This incipient AFM ordering occurs at the same point where an exponentially large number of different valence orderings become degenerate ($S = 0$ ground state sector). However, the presence of a triplon that propagates across the lattice could lead to two different scenarios for the bond correlations.

It can either select one particular valence bond ordering via an order by disorder mechanism, or simply destroy any long range bond ordering. In the former scenario, the application of a small magnetic field, B , that couples to the spins via the Zeeman term $-B \sum_{\mathbf{r}} S_{\mathbf{r}}^z$, should stabilize a particular bond ordering out of the exponentially large number of degenerate bond ordered ground states that exist at $B = 0$. The selection mechanism would be provided by the kinetic energy of the field induced triplons, which should be minimized for a particular bond ordered background. In this scenario, the selected bond ordering coexists with the AFM xy -ordering induced by the condensation of triplons at the single particle state with momentum $\mathbf{k} = (\pi, \pi)$. Figure 6 illustrates this situation for the bond ordering that has the highest susceptibility, according to the results that we discuss below. In the second scenario, the bond fluctuations induced by the triplon propagation are strong enough to produce a valence bond liquid with short-range bond-bond correlations. The only order parameter that survives is the AFM ordering which arises from the triplon condensation.

To further explore both scenarios, it is necessary to compute bond-bond correlation functions for the $S = S^z = 1$ ground state. We introduce the bond structure factor, $S_B(\mathbf{k}, \nu)$, for the local bond operator $B_{\mathbf{r}\nu} = \mathbf{s}_{\mathbf{r}} \cdot \mathbf{s}_{\mathbf{r}+\mathbf{e}_\nu}$. $\mathbf{k} = (k_x, k_y)$ is the wave vector, $\nu = \{x, y\}$, and \mathbf{e}_ν is the relative vector connecting nearest-neighbor spins along the ν -direction. Then,

$$S_B(\mathbf{k}, \nu) = \frac{1}{L_x L_y} \sum_{\mathbf{r}, \mathbf{r}'} e^{i\mathbf{k} \cdot (\mathbf{r} - \mathbf{r}')} \langle B_{\mathbf{r}\nu} B_{\mathbf{r}'\nu} \rangle. \quad (10)$$

The staggered bond ordering (SBO) shown in Fig. 6 should produce a sharp maximum in $S_B(\mathbf{k}, \nu)$ at $\mathbf{k} = (\pi, \pi)$. In contrast, the bond structure factors obtained for 4×4 , 6×6 lattices have very broad maxima at $\mathbf{k} = (\pi, \pi)$, indicating that the second scenario with short ranged bond correlations is more appropriate for the ($S = 1, S^z = 1$) ground state (see Fig. 7 a and b). The same scenario holds for the 4×40 lattice (Fig. 7 c). In this case, $S_B(\mathbf{k}, y)$ has an approximately degenerate line of maxima for $k_x = \pi/2$, indicating that bond correlations between adjacent vertical lines are very weak.

IV. APPLICATION TO A $D = 1$ ANISOTROPIC HEISENBERG MODEL WITH NNN INTERACTIONS

The one-dimensional family of spin-1/2 Hamiltonians introduced in Refs. [36] and [23] is

$$H_Q = \sum_{j;\nu=1,2} J_\nu \left[\Delta_\nu \left(s_{j+\nu}^z s_j^z - \frac{1}{4} \right) + s_{j+\nu}^x s_j^x + s_{j+\nu}^y s_j^y \right].$$

The Hamiltonian coefficients are parametrized by the single variable Q : $\Delta_\nu = \cos(\nu Q)$ and $J_1 = -4J_2 \cos Q$, with $0 \leq Q < \pi$. H_Q satisfies the FF property for all Q if we choose appropriate boundary conditions. In particular, for $Q = \pi/2$, the model reduces to two decoupled ferromagnetic Heisenberg chains whose exact solutions are known [37]. In this case, the ground-space dimension is $g = (L/2 + 1)^2$ or $g = (L + 3)(L + 1)/4$ for even or odd L , respectively.

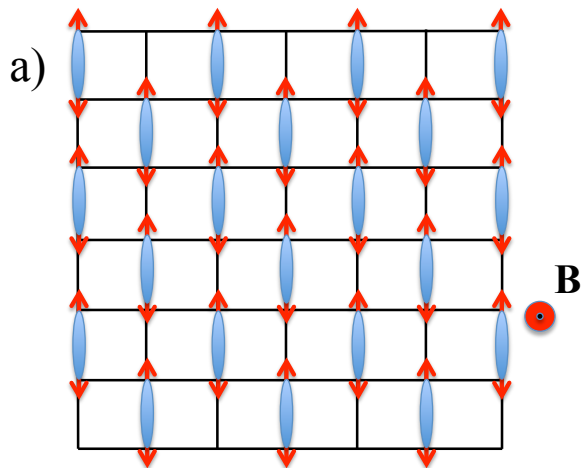


FIG. 6. Illustration of one of the possible scenarios in presence of a finite magnetic field \mathbf{B} . The ovals indicate that the corresponding bonds have a predominant singlet character. The staggered bond ordering (broken Z_4 symmetry) shown in the figure should produce a sharp maximum in the bond structure factor $S_B(\mathbf{k}, \nu)$ at $\mathbf{k} = (\pi, \pi)$. The arrows indicate the AFM ordering in the plane perpendicular to the applied magnetic field induced by the condensation of triplons. The staggered magnetization can point along any direction obtained by a global spin rotation along the field direction (broken $U(1)$ symmetry).

L is the number of spins in the chain. The analytical solutions for the ground states presented in Ref. [23] show that the ground space for $Q = \pi/2$ is continuously connected with the ground space for arbitrary Q . While, in principle, the ground-space degeneracy for arbitrary Q could be larger than that for $Q = \pi/2$, the ERM shows that such a degeneracy remains constant. Therefore, the ERM allows for an efficient computation of spin-spin correlations in any ground state of H_Q .

V. CONCLUSIONS

We introduced an exact renormalization method that obtains the full ground-space of Hamiltonians satisfying a frustration-free property. The method outputs a sequence of tensors whose contraction allows for the computation of correlation functions in any ground state. Such correlations can be used to characterize zero-temperature states of matter. The cost of the method depends on the ground state degeneracy for each renormalization step. The method computes the degeneracy and verifies the frustration-free property.

We applied the method to two spin systems. First, we considered a FF Hamiltonian in $D = 2$ whose ground-space dimension increases exponentially in the linear size of a square lattice. We applied the ERM successfully and characterized the physical properties of the only ground state with total spin $S = 1$ and projection $S^z = 1$. Such a ground state differs qualitatively from the (bond ordered) singlet ground states identified in Ref. [25]. In particular, it describes a quantum critical point associated with the onset of AFM ordering. Ac-

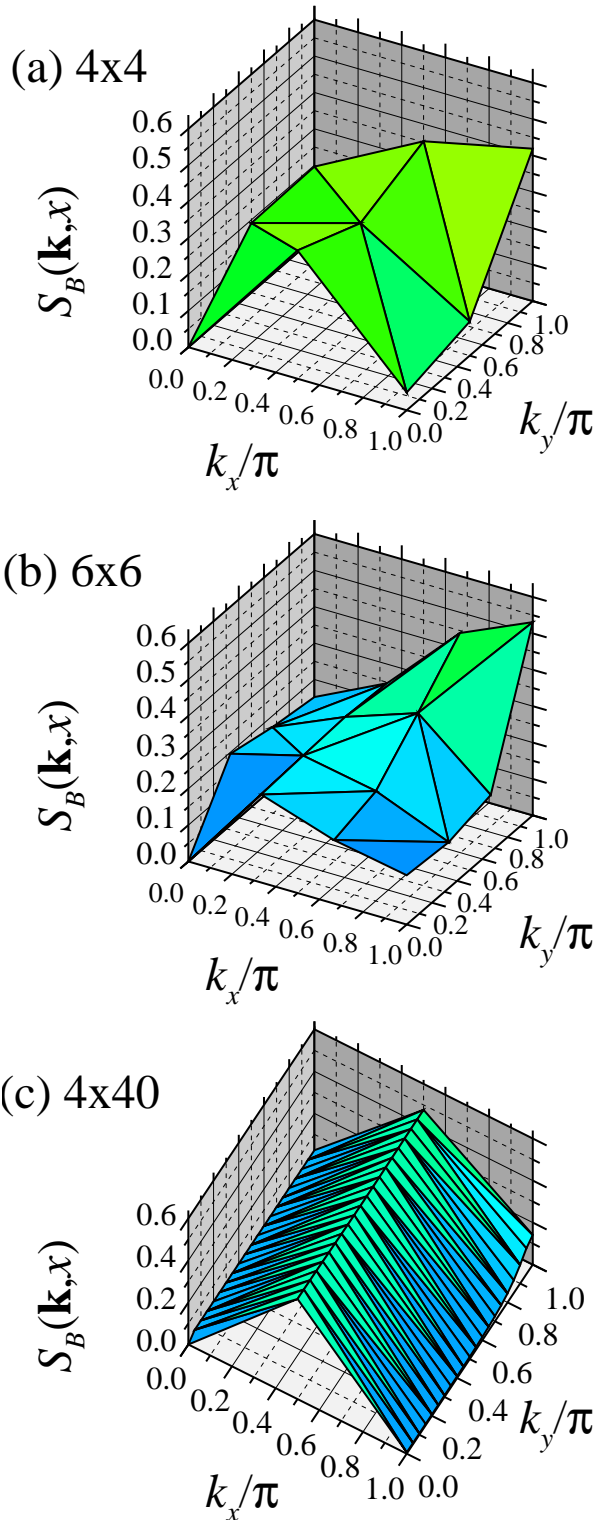


FIG. 7. Bond structure factors $S_B(\mathbf{k}, x)$ as a function of $\mathbf{k} = (k_x, k_y)$, computed with the ERM for different lattice sizes. a) $L_x = L_y = 4$. b) $L_x = L_y = 6$. c) $L_x = 4, L_y = 40$.

ording to our results, the application of an arbitrary small magnetic field $B > 0$ induces AFM order of the spin components that are orthogonal to field's direction. Our results also indicate that the finite magnetic field destroys any of the long-range bond orderings that compete at $B = 0$ [25].

We also applied the ERM to the one-dimensional family of FF spin-1/2 Hamiltonians described in Eq. (11). We verified that the ground space dimension is $g = (L/2 + 1)^2$ ($g = (L+3)(L+1)/4$) for even (odd) L , as conjectured in Ref. [23]. The ERM is efficient in this case.

Both applications illustrate the power of the ERM for obtaining exact ground state properties of frustration free Hamiltonians. Nevertheless, our renormalization method can also be used in more general contexts. For example, since stochastic matrices can be sometimes related to FF Hamiltonians [38], the ERM can be used to compute properties of (classical) systems in and out of equilibrium. Similarly, the ERM can be used to solve combinatorial optimization problems [39].

VI. ACKNOWLEDGEMENTS

Work at LANL was performed under the auspices of the U.S. DOE contract No. DE-AC52-06NA25396 through the LDRD program. AEF thanks NSF for funding under grant No. DMR-0955707. RDS thanks NSF for funding under the CCF program.

Appendix A: Exactness and cost of the ERM

We provide more details about the ERM, showing the exactness of the method and estimating the computational requirements. With no loss of generality π_{v_k} is

$$\pi_{v_k} = \sum_{\alpha=1}^{A_k} O_{k,\alpha}^{w_{k(1)}} \otimes \dots \otimes O_{k,\alpha}^{w_{k(r)}}, \quad (\text{A1})$$

where \otimes is the tensor product. The sets $w_{k(j)}$ satisfy $w_{k(j)} \cap v_k \neq \{\emptyset\}$. Any state $|i^{v_k}\rangle$ corresponds to a particular state $|i^{w_{k(1)}}, \dots, i^{w_{k(r)}}\rangle$ for the sets $w_{k(j)}$ in v_k . We assume then a specification of H via access to $\Pi_H(\cdot)$ that, on input (v_k, i, i') , it outputs all the matrix elements

$$\langle i^{w_{k(i)}} | O_{k,\alpha}^{w_{k(j)}} | i^{w_{k(i)}} \rangle, \quad (\text{A2})$$

for $1 \leq j \leq r$ and $1 \leq \alpha \leq A_k$. Π_H also outputs all the sets $w_{k(j)}$ involved in each term of the decomposition of π_{v_k} . In other words, Π_H gives all the information about the action of each term of π_{v_k} in the states $|i^{v_k}\rangle$. Such a Hamiltonian specification is common in applications, e.g. a spin-1/2 system specified in terms of Pauli operators. The actual computational cost of the ERM should consider the number of times that Π_H is used, which is typically linear in p .

Our renormalization method takes the ordered set $\{v_1, \dots, v_p\}$ as input and uses Π_H . It outputs a bit b denoting whether H is frustration free ($b = 0$) or not ($b = 1$) [40]. If $b = 0$, the ERM also outputs the ground states specified by

a sequence of tensors T_l or T_l^\dagger – see Eq. (3). Because Eq. (3) involves a summation over repeated indexes, we use Einstein notation in the following. For $l = 1, \dots, p$, T_l is determined by its (complex) entries:

$$T_l := \begin{cases} (t_1)_{i^{w_1}}^{i^{z_1}} & \text{if } l = 1 \\ (t_l)_{i^{z_{l-1}}, i^{w_l}}^{i^{z_l}} & \text{if } l > 1 \end{cases}, \quad (\text{A3})$$

with $1 \leq i^{w_l} \leq d_{w_l}$, $1 \leq i^{z_l} \leq g_l$, and g_l determined by the ERM (see below). For each $i^{z_l} \leq g_l$, the vectors $|\psi_{i^{z_l}}^l\rangle = T_1^\dagger \bullet \dots \bullet T_l^\dagger |i^{z_l}\rangle$ are in \mathcal{H}_{z_l} and thus have d_{z_l} components in the computational basis. We recall that $z_l = \cup_{k=1}^l w_k$. Then, each such component is determined by i^{w_1}, \dots, i^{w_l} corresponding to the sets w_1, \dots, w_l , respectively. That is, $\{i^{w_1}, \dots, i^{w_l}\}$, with $1 \leq i^{w_k} \leq d_{w_k}$, also defines a computational basis for \mathcal{H}_{z_l} . The components of $|\psi_{i^{z_l}}^l\rangle$ in such a basis are

$$(u_1)_{i^{z_1}}^{i^{w_1}} (u_2)_{i^{z_2}}^{i^{w_2}} \dots (u_l)_{i^{z_l}}^{i^{w_l}}, \quad (\text{A4})$$

with

$$(u_1)_{i^{z_1}}^{i^{w_1}} = ((t_1)_{i^{w_1}}^{i^{z_1}})^* \quad (\text{A5})$$

$$(u_k)_{i^{z_k}}^{i^{w_k}} = ((t_k)_{i^{z_{k-1}}, i^{w_k}}^{i^{z_k}})^*, \quad 2 \leq k \leq p.$$

In particular, when $l = p$, we have $z_p = \mathcal{V}$ and Eq. (A4) defines the contraction in Eq. (3). This contraction is associated with a tree-like tensor network – see Fig 2 for an example.

For $l = 1$, we denote by γ_1 the d_{v_1} -dimensional matrix representation of π_{v_1} in $\mathcal{H}_{v_1} = \mathcal{H}_{w_1}$, in the computational basis. The ERM constructs γ_1 using Π_H once. Then, the ERM performs *exact* diagonalization to obtain g_1 and an orthonormal vector basis $\{|\phi_{i^{z_1}}^1\rangle\}_{1 \leq i^{z_1} \leq g_1}$ for the zero-eigenvalue eigenvectors of γ_1 . T_1 is the tensor that maps such eigenvectors to vectors or states in the computational basis:

$$T_1 = \sum_{i^{z_1}=1}^{g_1} |i^{z_1}\rangle \langle \phi_{i^{z_1}}^1|. \quad (\text{A6})$$

The entries of T_1 are

$$(t_1)_{i^{w_1}}^{i^{z_1}} = \langle \phi_{i^{z_1}}^1 | i^{w_1} \rangle, \quad (\text{A7})$$

with $1 \leq i^{w_1} \leq d_{w_1}$ and $1 \leq z_1 \leq g_1$.

In the l -th step, $l \geq 2$, the ERM uses Π_H to construct the $h_l \times h_l$ matrix γ_l , $h_l = g_{l-1} d_{w_l}$, with entries

$$\gamma_l \rightarrow \langle \phi_{i^{z_{l-1}}}^{l-1}, i^{w_l} | \pi_{v_l} | \phi_{i^{z_{l-1}}}^{l-1}, i^{w_l} \rangle. \quad (\text{A8})$$

Here, $i^{z_{l-1}}, i^{w_l} = 1, \dots, g_{l-1}$ and $i^{w_l}, i^{w_l} = 1, \dots, d_{w_l}$. The ERM performs exact diagonalization of γ_l and continues only if the lowest eigenvalue is 0 ($b = 0$). It computes the multiplicity of the zero eigenvalue, assigns it to g_l , and computes a complete orthonormal basis of h_l -dimensional eigenvectors $\{|\phi_{i^{z_l}}^l\rangle, \dots, |\phi_{i^{z_l}}^l\rangle\}$ for the zero eigenvalue. The ERM assigns the tensor T_l to the transformation that maps such eigenvectors to vectors in the computational basis of \mathcal{H}_{z_l} :

$$T_l = \sum_{i^{z_l}=1}^{g_l} |i^{z_l}\rangle \langle \phi_{i^{z_l}}^l|. \quad (\text{A9})$$

The entries of T_l are

$$(t_l)_{i^{z_{l-1}}, i^{w_l}} = \langle \phi_{i^{z_l}}^l | i^{z_{l-1}}, i^{w_l} \rangle. \quad (\text{A10})$$

To show that the ERM is exact, we first remark that the eigenvectors $|\phi_{i^{z_l}}^l\rangle$ represent the states $|\psi_{i^{z_l}}^l\rangle$, as determined by Eq. (A4). Then, we will show that the states

$$|\psi_{i^{z_l}}^l\rangle = T_1^\dagger \bullet \dots \bullet T_l^\dagger |i^{z_l}\rangle, \quad (\text{A11})$$

given according to Eq. (A4), are ground states of $H_l = \sum_{k=1}^l \pi_{v_k}$ for all $l \in \{1, 2, \dots, p\}$, when H_l are frustration free.

The proof is inductive. For $l = 1$, $|\phi_{i^{z_1}}^1\rangle = |\psi_{i^{z_1}}^1\rangle$ is a ground state of γ_1 or $\pi_{v_1} = H_1$ by definition. That is, $|\psi_{i^{z_1}}^1\rangle$, as determined from Eq. (A4), is a ground state of H_1 for each $i^{z_1} = 1, \dots, g_1$. We assume now that

$$\{|\psi_{i^{z_{l-1}}}^{l-1}\rangle = T_1^\dagger \bullet \dots \bullet T_{l-1}^\dagger |i^{z_{l-1}}\rangle\}_{1 \leq i^{z_{l-1}} \leq g_{l-1}}$$

is an orthogonal basis for the ground subspace of H_{l-1} . Then, if $|\phi\rangle$ is a ground state of H_l ,

$$|\phi\rangle = \sum_{i^{z_{l-1}}=1}^{g_{l-1}} \sum_{i^{w_l}=1}^{d_{w_l}} c_{i^{z_{l-1}}, i^{w_l}} |\psi_{i^{z_{l-1}}}^{l-1}, i^{w_l}\rangle \quad (\text{A12})$$

with $c_{i^{z_{l-1}}, i^{w_l}}$ complex amplitudes. Otherwise, $|\phi\rangle$ would not belong to the intersection between the ground subspaces of H_{l-1} and H_l , a requirement for frustration-free Hamiltonians. It suffices to obtain γ_l , a projection of π_{v_l} into the subspace spanned by $\{|\psi_{i^{z_{l-1}}}^{l-1}, i^{w_l}\rangle\}_{1 \leq i^{z_{l-1}} \leq g_{l-1}, 1 \leq i^{w_l} \leq d_{w_l}}$. Without loss of generality, we can choose a value of i^{z_l} such that

$$|\phi\rangle = |\phi_{i^{z_l}}^l\rangle. \quad (\text{A13})$$

Thus,

$$c_{i^{z_{l-1}}, i^{w_l}} = (u_l)_{i^{z_{l-1}}, i^{w_l}}^{i^{z_l}}, \quad (\text{A14})$$

where $(u_l)_{i^{z_{l-1}}, i^{w_l}}^{i^{z_l}}$ are the entries of T_l^\dagger . That is,

$$\begin{aligned} |\phi\rangle &= (u_l)_{i^{z_{l-1}}, i^{w_l}}^{i^{z_l}} |\psi_{i^{z_{l-1}}}^{l-1}, i^{w_l}\rangle \\ &= (u_1)_{i^{z_1}}^{i^{z_1}} (u_2)_{i^{z_2}}^{i^{z_2}} \dots (u_l)_{i^{z_l}}^{i^{z_l}} |i^{w_1}, \dots, i^{w_l}\rangle. \end{aligned} \quad (\text{A15})$$

The contraction in Eq. (A15) coincides with that of Eq. (A4). It follows that

$$|\phi\rangle = |\psi_{i^{z_l}}^l\rangle = T_1^\dagger \bullet \dots \bullet T_l^\dagger |i^{z_l}\rangle \quad (\text{A16})$$

is a ground state of H_l for all $1 \leq i^{z_l} \leq g_l$. In particular, $|\psi_{i^{z_p}}^p\rangle$, with $1 \leq i^{z_p} \leq g_p = g$, are all the ground states of H .

1. Computational requirements

We let N_T be the total cost, i.e., the total number of elementary operations to obtain all entries of T_1, \dots, T_p . For simplicity, we do not consider in the cost the number of queries to Π_H , which is typically linear in p . We also let M_T be

the memory requirements, i.e., the number of coefficients that need to be kept in memory during the implementation of the ERM.

We first write

$$N_T = \sum_{l=1}^p N_T^l, \quad M_T = \sum_{l=1}^p M_T^l. \quad (\text{A17})$$

To obtain T_1 , the ERM performs exact diagonalization of γ_1 . Because γ_1 is of dimension d_{w_1} , the cost of obtaining its eigenvectors and eigenvalues is $N_T^1 \leq EV(d_{w_1}) \in \mathcal{O}(\text{poly}(d_{w_1}))$. $EV(d)$ is the cost of exact diagonalization of a $d \times d$ matrix, which is almost quadratic in d in actual implementations. Only the g_1 eigenvectors with zero eigenvalue need to be kept in memory for the following step and thus $M_T^1 \propto g_1 d_{w_1}$.

The cost of obtaining all zero-eigenvalue eigenvectors of γ_l is bounded by $EV(h_l)$. To obtain N_T^l we need to add the cost of computing γ_l . Each matrix element of γ_l in Eq. (A8) is

$$\begin{aligned} \langle i^{z_{l-1}} | \langle i^{w_l} | T_{l-1} \bullet \dots \bullet T_1 \bullet \pi_{v_l} \bullet \\ \bullet T_1^\dagger \bullet \dots \bullet T_{l-1}^\dagger |i^{z_{l-1}}\rangle |i^{w_l}\rangle. \end{aligned} \quad (\text{A18})$$

We consider the decomposition in Eq. (A1) and we are interested in obtaining the cost of computing a particular term

$$\begin{aligned} \langle i^{z_{l-1}} | \langle i^{w_l} | T_{l-1} \bullet \dots \bullet T_1 \bullet \left(O_{k,\alpha}^{w_{k(1)}} \otimes \dots \right. \\ \left. \dots \otimes O_{k,\alpha}^{w_{k(r)}} \right) \bullet T_1^\dagger \bullet \dots \bullet T_{l-1}^\dagger |i^{z_{l-1}}\rangle |i^{w_l}\rangle. \end{aligned} \quad (\text{A19})$$

We can interleave trivial operators $\mathbb{1}_w = \sum_{i^w=1}^{d_w} |i^w\rangle \langle i^w|$ in Eq. (A19) for those $w \neq w_{k(j)}$ without affecting the output of the contraction. That is, we extend the definition of $O_{k,\alpha}^{w_{k(j)}}$ so that $O_{k,\alpha}^{w_{k(j)}} = \mathbb{1}_{w_{k(j)}}$ for $r < j \leq l$. Then we write

$$(o_j)_{i^{w_{k(j)}}}^{i^{w_{k(j)}}} = \langle i^{w_{k(j)}} | O_{k,\alpha}^{w_{k(j)}} | i^{w_{k(j)}} \rangle \quad (\text{A20})$$

for all $1 \leq j \leq l$. Equation (A19) is

$$\begin{aligned} (t_1)_{i^{w_1}}^{i^{z_1}} \dots (t_{l-1})_{i^{z_{l-2}}, i^{w_{l-1}}}^{i^{z_{l-1}}} \left[(o_1)_{i^{w_1}}^{i^{w_1}} \dots \right. \\ \left. (o_l)_{i^{w_l}}^{i^{w_l}} \right] (u_1)_{i^{z_1}}^{i^{z_1}} \dots (u_{l-1})_{i^{z_{l-1}}}^{i^{z_{l-1}}}, \end{aligned} \quad (\text{A21})$$

where we used Eq. (A4). As before, Eq. (A21) refers to a contraction of a tree-like tensor network; see Fig. 8 for an example.

The cost of evaluating Eq. (A21) depends on the support of v_l , that is, the number and position of spins that belong to v_l . This is so because Eq. (A21) can be sometimes simplified considering that

$$T_k T_k^\dagger = \sum_{i^{z_k}=1}^{g_k} |i^{z_k}\rangle \langle i^{z_k}| \quad (\text{A22})$$

and then

$$(t_k)_{i^{z_{k-1}}, i^{w_k}}^{i^{z_k}} (u_k)_{i^{z_k}}^{i^{z_{k-1}}, i^{w_k}} = \delta_{i^{z_k}, i^{z_{k-1}}} \quad (\text{A23})$$

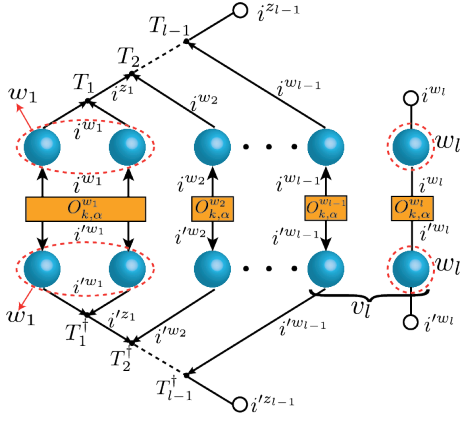


FIG. 8. Representation of the network contraction for each matrix element of γ_l in Eq. (A21) for the same system of Fig. 2. Blue circles are spins. π_{v_l} is a sum of A_k terms of the form $O_{k,\alpha}^{w_1} \otimes \dots \otimes O_{k,\alpha}^{w_l}$, and some $O_{k,\alpha}^{w_j}$ may act trivially in w_j ; i.e., $O_{k,\alpha}^{w_j} = \sum_{i^{w_j}=1}^{d_{w_j}} |i^{w_j}\rangle \langle i^{w_j}|$. Arrows denote a sum of the index in the corresponding edge. Open circles denote a fixed index, referring to a particular matrix element of γ_l , the projection of π_{v_l} in the ground subspace of $H_{l-1} = \sum_{k=1}^{l-1} \pi_{v_k}$. $1 \leq i^{w_l}, i'^{w_l} \leq d_{w_l}$ and $1 \leq i^{z_{l-1}}, i'^{z_{l-1}} \leq g_{l-1}$.

which are useful if $O_{k,\alpha}^{w_{k(j)}} = \mathbb{1}_{w_{k(j)}}$. Nevertheless, to analyze the cost of computing Eq. (A21) we consider the worst case scenario in which $O_{k,\alpha}^{w_{k(j)}} \neq \mathbb{1}_{w_{k(j)}}$ for all $1 \leq j \leq l$. We can rearrange the sum and compute Eq. (A21) in l sequential steps as follows. First, we compute the

$$(t_1)_{i'^{z_1}}^{i^{z_1}} (o_1)_{i'^{w_1}}^{i^{w_1}} (u_1)_{i^{z_1}}^{i^{w_1}}$$

for all $1 \leq i^{z_1}, i'^{z_1} \leq g_1$. Because $1 \leq i^{w_1}, i'^{w_1} \leq d_{w_1}$, this step has cost $\propto (d_{w_1} g_1)^2$. We keep the computed values in memory. Next we compute the

$$(t_1)_{i'^{z_1}}^{i^{z_1}} (o_1)_{i'^{w_1}}^{i^{w_1}} (u_1)_{i^{z_1}}^{i^{w_1}} (t_2)_{i'^{z_2}}^{i^{z_2}} (o_2)_{i'^{w_2}}^{i^{w_2}} (u_2)_{i^{z_2}}^{i^{w_2}}$$

for all $1 \leq i^{z_2}, i'^{z_2} \leq g_2$. This step has an additional cost $\propto (g_1 d_{w_2} g_2)^2$, where the first g_1 comes from the sum in i^{z_1} and i'^{z_1} . We keep implementing the procedure sequentially until we compute

$$(t_1)_{i'^{z_1}}^{i^{z_1}} (o_1)_{i'^{w_1}}^{i^{w_1}} (u_1)_{i^{z_1}}^{i^{w_1}} \dots \quad (A24)$$

$$\dots (t_{l-1})_{i'^{z_{l-1}}}^{i^{z_{l-1}}} (o_{l-1})_{i'^{w_{l-1}}}^{i^{w_{l-1}}} (u_{l-1})_{i^{z_{l-1}}}^{i^{w_{l-1}}},$$

which has an additional cost $\propto (h_{l-1} g_{l-1})^2$ with respect to the previous computations. That is, the sequential method has an overall cost $\propto \sum_{k=1}^{l-1} (h_k \cdot g_k)^2$, with $g_0 = 1$. The sequential method can be understood from the example in Fig. 8, in which the sequential steps regard the contraction of tensors from left to right.

The last step is to compute

$$(o_l)_{i'^{w_l}}^{i^{w_l}} \quad (A25)$$

for all $1 \leq i^{w_l}, i'^{w_l} \leq d_{w_l}$. This step is implemented using Π_H and has no cost under our assumption. Then, the

computation of Eq. (A21) for all $1 \leq i^{w_l}, i'^{w_l} \leq d_{w_l}$ and $1 \leq i^{z_{l-1}}, i'^{z_{l-1}} \leq g_{l-1}$ can be implemented with

$$\propto \sum_{k=1}^{l-1} (g_{k-1} d_{w_k} \cdot g_k)^2 \quad (A26)$$

elementary operations. To compute γ_l , we need to add a multiplicative factor A_l that regards the number of terms in the decomposition of π_{v_l} . Then,

$$N_T^l = EV(g_{l-1} d_{w_l}) + c A_l \sum_{k=1}^{l-1} (h_k \cdot g_k)^2, \quad (A27)$$

with $c > 1$ a constant. A memory of $M_T^l \propto h_l g_l$ is needed for the ground states of γ_l .

Typically, A_l is bounded by some constant A . In this case,

$$N_T \propto \sum_{k=1}^p EV(h_k) + (p-1)(d_{w_1} g_1)^2 + (p-2)(h_2 g_2)^2 + \dots + (h_{p-1} g_{p-1})^2. \quad (A28)$$

In addition,

$$M_T \propto \sum_{k=1}^p h_k g_k. \quad (A29)$$

If $g_k \in \mathcal{O}[\text{poly}(p)]$ and $d_{w_k} \in \mathcal{O}[\text{poly}(p)]$, then $N_T \in \mathcal{O}[\text{poly}(p)]$ and the ERM is efficient.

2. Optimal cost

The total cost of the ERM in Eq. (A28) depends on d_{w_l} and g_l . In many applications, d_{w_l} is constant and N_T and M_T are functions of g_1, \dots, g_p . The cost can then be minimized by considering all possible orderings of w_1, \dots, w_p such that N_T and/or M_T are minimum. This procedure rules out some possible orderings that yield exponential complexity in systems in which the ERM could be implemented efficiently. For example, consider a square spin lattice and assume that the terms π_{v_k} in the Hamiltonians involve two nearest-neighbor spins in either direction. The ERM could be implemented to obtain the ground states of each chain along a particular direction and then add the Hamiltonian terms in the other direction. However, this construction results in exponential complexity if the ground space of each chain is degenerate because the number of ground states that have to be kept in memory is exponentially large in the length of the chains. A more efficient choice considers “growing” the system using the “snake” path depicted in Fig. 3 (b).

In a different example we consider a binary tree of depth q and assume $p = 2^q$. Each node in the basis of the tree corresponds to a single spin in a lattice. A standard real-space renormalization method for such a binary tree will have $l = 1, \dots, q$ steps, each involving a diagonalization of 2^{q-l} matrices of dimension g_{2^l} each. The memory requirement for such method is dominated by the last step, which requires

dealing with a subspace of dimension $g_{p/2} \times g_{p/2}$, spanned by all the ground states obtained in the previous step. In addition, each such ground state has $(g_{p/4})^2$ components in a computational basis. If $g_k \propto k^\beta$, the memory requirement

to implement the last step is $M'_T \in \mathcal{O}[p^{4\beta}]$. Nevertheless, our ERM implies $M_T \in \mathcal{O}(p^{2\beta})$ in this case. Clearly, $M'_T \gg M_T$ when $\beta > 0$, $p \gg 1$. The standard renormalization method may outperform the ERM only if $\beta = 0$.

-
- [1] K.G. Wilson, Rev. Mod. Phys. 47, 773 (1975).
- [2] R. Bulla, T. A. Costi and T. Pruschke, Rev. Mod. Phys. **80**, 395 (2008).
- [3] J. Kondo, Prog. Theor. Phys. **32**, 37 (1964).
- [4] S.R. White, Phys. Rev. Lett. 69, 2863 (1992).
- [5] Simeng Yan, David A. Huse, and Steven R. White, Science **332** 1173 (2011).
- [6] P. Corboz, S. R. White, G. Vidal, M. Troyer, Phys. Rev. B **84**, 041108 (2011).
- [7] S. Depenbrock, I. P. McCulloch, U. Schollwöck, Phys. Rev. Lett. **109**, 067201 (2012).
- [8] H.-C. Jiang, H. Yao, L. Balents, Phys. Rev. B **86**, 024424 (2012).
- [9] F. Verstraete and J. I. Cirac, cond-mat/0407066. V. Murg, F. Verstraete, and J. I. Cirac, Phys. Rev. A **75**, 033605 (2007).
- [10] Hamed Saberi, Andreas Weichselbaum, and Jan von Delft, Phys. Rev. B **78**, 035124 (2008).
- [11] Guifre Vidal, Phys. Rev. Lett. **99**, 220405 (2007), G. Evenbly, G. Vidal, Phys. Rev. B **79**, 144108 (2009).
- [12] Glen Evenbly, Guifre Vidal, Phys. Rev. Lett. **102**, 180406 (2009).
- [13] G. Sierra and M. A. Martn-Delgado, cond-mat/9811170 (preprint); Y. Nishio, N. Maeshima, A. Gendiar, and T. Nishino, cond-mat/0401115.
- [14] Zheng-Cheng Gu, Michael Levin, Xiao-Gang Wen, Phys. Rev. B **78**, 205116 (2008).
- [15] Z. Y. Xie, H. C. Jiang, Q. N. Chen, Z. Y. Weng, T. Xiang, Phys.Rev.Lett. **103** 160601 (2009).
- [16] H.H. Zhao, Z.Y. Xie, Q.N. Chen, Z.C. Wei, J.W. Cai, T. Xiang, Physical Review B **81**, 174411 (2010).
- [17] H.-C. Jiang, Z. Wang, L. Balents, Nature Phys. **8**, 902-905 (2012).
- [18] D. Perez-Garcia, F. Verstraete, M.M. Wolf, and J.I. Cirac, Quantum Information and Computation **8**, 650 (2008).
- [19] S. Bravyi and B. Terhal, SIAM J. Comp. **39**, 1462 (2009)
- [20] R.D. Somma and S. Boixo, e-print arXiv:1110.2494 (2011).
- [21] I. Affleck, T. Kennedy, E.H. Lieb, and H. Tasaki, Phys. Rev. Lett. **59**, 799 (1987).
- [22] D. Aharonov, W. Van Dam, J. Kempe, Z. Landau, S. Lloyd, and O. Regev, in Proc. of the 45th Annual IEEE Symp. on Found. Comp. Sci., 42 (2004).
- [23] C. D. Batista and R. D. Somma, Phys. Rev. Lett. 109, 227203 (2012).
- [24] G. H. Wannier, Phys. Rev. **79**, 357 (1950).
- [25] C. D. Batista and S. Trugman, Phys. Rev. Lett. **93**, 217202 (2004).
- [26] M. Lajkó, P. Sindzingre, and K. Penc, Phys. Rev. Lett. 108, 017205 (2012).
- [27] S. Bravyi. Contemporary Mathematics **536**, 2011.
- [28] N. de Beaudrap, M. Ohliger, T.J. Osborne, and J. Eisert, Phys. Rev. Lett. **105**, 060504 (2010).
- [29] Hong-Hao and Mikel Sanz, Phys. Rev. B **82**, 104404 (2010).
- [30] The ERM also works if \mathcal{V} corresponds to a set of sites that can be occupied by a limited number of particles like fermions or bosons [31].
- [31] P. Jordan and E. P. Wigner, Z. Phys. 47, 631 (1928).
- [32] Note that, by using the superscript x , we also clarify the Hilbert space to which $|i^x\rangle$ belongs to.
- [33] G. Vidal, Phys. Rev. Lett. **99**, 220405 (2007).
- [34] G. Evenbly and G. Vidal, e-print arXiv:1205.0639 (2012).
- [35] Karlo Penc, private communication.
- [36] C. D. Batista, Phys. Rev. B 80, 180406 (2009).
- [37] H. Bethe, Z. für Physik A **71**, 205 (1931).
- [38] C.L. Henley, J. of Phys: Cond.Mat. **16**, S891 (2004). C. Castellano, C. Chamon, C. Murphy, and P. Pujol, Ann. of Phys. **318**, 316 (2005). F. Verstraete, M. M. Wolf, D. Perez-Garcia, and J. I. Cirac, Phys. Rev. Lett. **96**, 220601 (2006).
- [39] R.D. Somma, C.D. Batista, and G. Ortiz, Phys. Rev. Lett. **99**, 030603 (2007).
- [40] If H is *almost* frustration free, our renormalization method may still provide a good approximation to the ground states. In this case, an upper bound to the error can be computed by the method.